Citation: Pineda, K., T. Hayashida (2022), S-wave velocities estimation using seismic ambient noise analysis at San Miguel Volcano, El Salvador, Synopsis of IISEE-GRIPS Master's Thesis.

S-WAVE VELOCITIES ESTIMATION USING SEISMIC AMBIENT NOISE ANALYSIS AT SAN MIGUEL VOLCANO, EL SALVADOR

Kevyn Enrique Pineda Ortiz[1] **Supervisor: Takumi HAYASHIDA**[2]
MEE21703

ABSTRACT

San Miguel volcano is one of the most active volcanoes in El Salvador. However, its structural properties are not fully understood. Four broadband seismometers were deployed by the Ministry of Environment of El Salvador from February 2014 to April 2014. We analyzed continuous ambient noise data (>0.2 Hz) using the spatial autocorrelation (SPAC) method and seismic interferometry technique, assuming the ambient noise is uniform both in time and space. The SPAC technique enabled us to obtain the phase velocity of surface waves from 0.2 to 1.0 Hz. We also determined Rayleigh-wave group velocities with seismic interferometry, which exploits Green's function from the cross-correlation of ambient noise recordings for each sensor-to-sensor pair. The combined use of the two methods offered ways to gain information about the shallow to deep seismic velocity structure from the same dataset. Through a joint inversion procedure, which included phase and group velocities, we estimated a velocity structure composed of four layers with shear wave velocities in the range of 1.0 km/s – 2.8 km/s. We located 15 volcano-tectonic earthquakes using the velocity model, resulting in a better-constrained hypocenter location. The hypocenter locations coincide with a deformation zone, known as the San Miguel Zone Fault, on the volcano's northern flank.

Keywords: SPAC method, Seismic Interferometry, Velocity structure, volcano.

1. INTRODUCTION

El Salvador is located in the northern part of Central America and extends along the Pacific coast, including part of the convergent Cocos-Caribbean plate boundary. The tectonic setting of El Salvador is controlled by the movements of the North American plate, Cocos plate, and Caribbean plate, but the seismic activity in El Salvador is associated mainly with the subduction of the Cocos plate beneath the Caribbean plate.

The volcanic chain in El Salvador runs parallel to the subduction zone. Six volcanoes in El Salvador are considered active due to their recent eruptions and fumarolic activity: Santa Ana, Izalco, San Salvador, Ilopango, San Vicente, Berlin, and San Miguel volcanoes. San Miguel volcano is located in the eastern region of El Salvador and is considered one of the most active volcanos in the country. The volcano, its height is 2130 meters, is a high symmetrical stratovolcano that extends over approximately 190 km^2. Its main crater measures 800 meters in diameter and 340 meters in depth. Several cones had been built during its eruptions.

In recent years, the volcanic activity of the San Miguel volcano has been presented as scatter events, including ash and gas plumes emissions. Despite the recent volcano activity, the lack of investigations

[1] Ministry of Environment and Natural Resources (MARN), El Salvador.
[2] International Institute of Seismology and Earthquake Engineering, Building Research Institute.

on the structural properties of the volcano makes it hard to consider strategies for risk reduction. To determine the seismic velocity structure of the San Miguel volcano for determining accurate seismic events associated with its activity, we applied seismic interferometry and the Spatial Autocorrelation (SPAC) method. We analyzed the ambient seismic noise recorded by four broadband stations to estimate a local S-wave velocity structure model beneath the volcano and interpreted the seismicity associated with the volcano and its location.

2. DATA

We used seismic ambient noise data recorded at the San Miguel volcano broadband stations. After the last eruption in December 2014, the Ministry of Environment and Natural Resources of El Salvador (MARN) established a temporary seismic network to monitor the seismic activity associated with volcanic activity. The temporary network was located mainly on the northern flank of the San Miguel volcano (Figure 1), and continuous observation was performed from February 2014 to April 2014. The interstation distance is from 1.5 km to 5.5 km.

Since the sensors were installed on the ground surface, their record was affected considerably by signals with high-frequency content, such as wind, vehicles, or even volcanic signals

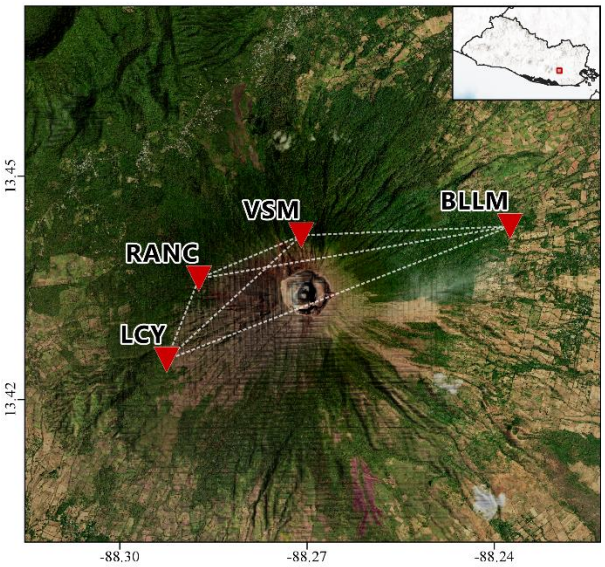

Figure 1. Distribution of the seismic station in the San Miguel volcano. The dotted white line represents the interstation path

3. METHODOLOGY

3.1. Microtremor analysis

The microtremor method studies the behavior of the surface waves and their spectra to infer the properties of the earth's shallow surface. Seismic sensors measure the velocity of the seismic waves propagating on the surface, and from the microtremor records, the derivation of the shear-wave velocity-depth relation is obtained. The microtremor analysis seeks to measure the dispersion curve of the surface waves, which represents the relation between the velocity of the wave at a certain depth, to obtain a layered-earth model of the velocity properties by performing an inverse analysis (Asten et al., 2018).

3.3.1. Seismic ambient noise

Actual broadband seismic sensors are sensitive enough to measure background ambient seismic noise and weak seismic signals caused by earthquakes. The ambient field vibrations are produced by several sources, including human activity and natural phenomena. The lack of recognizable content in the vibration signals has led the ambient field to be classified as 'seismic ambient noise' (Nakata et al., 2019).

3.3.2. Spatial autocorrelation method

The Spatial Autocorrelation (SPAC) method (also known as Aki's spatial autocorrelation method) provides a robust process to infer the properties of the subsurface structure using the relation between the spectrum of the seismic waves in time and their spectrum in space. Aki (1957) explained that the

phase-velocity of the surface waves could be obtained from the azimuthal average of the cross-correlation of microtremor measurements considering an azimuth average.
Aki (1965) defined the spatial autocorrelation coefficient $\rho(r,\omega)$, also known as a theoretical SPAC coefficient, as a function of the frequency for a given interstation distance (r) and an angular frequency over an azimuth averaged:

$$\rho(r,\omega) = \frac{1}{2\pi\ \Phi(\mathrm{r}=0,\omega)} \int_0^{2\pi} \Phi(r,\theta,\omega)\, d\theta \qquad (1)$$

The SPAC method proposes a technique to determine the phase velocity $c(\omega)$ of the dispersion curve from the analysis of ambient seismic noise using Eq. 2, which presents the relation of the phase velocity and Bessel function of the first kind and order zero J_0

$$\rho(r,\omega) = J_o\left(\frac{r\omega}{c}\right) \qquad (2)$$

3.3.3. Seismic interferometry

While the SPAC method studies the microtremor in the frequency domain, the seismic interferometry method analyzes the microtremor in the time domain. The term 'seismic interferometry (SI)' refers to the principle of generating a virtual seismic signal by the cross-correlation of seismic waveforms (coda-waves, seismic ambient noise) recorded at two different receivers (Wapenaar et al., 2006). The primary purpose of SI is to obtain information about the Green's function (G) (i.e., ground property) between two seismic stations using the correlation (C) of the recorded waveforms using Eq. 3.

$$C(x_a,x_b) = \frac{\alpha^2}{2}\frac{d}{dt}[G(x_a,x_b,t) - G(x_a,x_b,-t)] \qquad (3)$$

where α represents the normalization factor assuming the equipartition of the ambient wavefield.

4. ANALYSIS AND RESULTS

4.1. Spatial autocorrelation method

The SPAC coefficients (also called 'coherence') (Eq. 1) were calculated using only the vertical components of the ambient noise and for every individual station pair. The procedure was conducted for all the frequencies from 0.1 to 10 Hz. A marked decrease in the SPAC coefficients at high frequencies was observed. At high frequencies, the wavelength becomes much smaller than the interstation distance causing an increased attenuation. Moreover, at high frequencies, the scattering is higher, which causes a low signal-to-noise ratio (SNR). The maximum coherence of the curves occurs at frequencies smaller than 0.4 Hz. Thus, the phase velocity measurement is limited at low frequencies. However, we applied the approach Ekström et al. (2009) established, which allowed us to increase the frequency range of phase velocity measurements considering the SPAC coefficients' zero-crossing points. As a result, the phase velocity was calculated at frequencies from 0.1 to 1 Hz.

4.2. Seismic interferometry

Green's function was constructed by cross-correlating between all component combinations, including the radial (R) and traverse (T) components, as well as the vertical (Z) component. The data processing was done using a software package developed by T. Hayashida, and it followed the methodology proposed by Bensen et al. (2007).

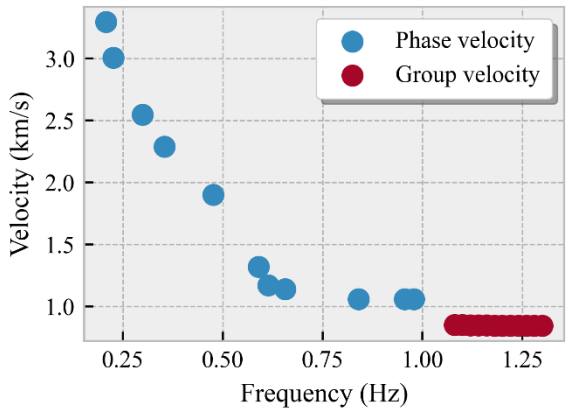

Figure 2. Estimated Rayleigh wave dispersion curve.

To increase the power of the surface wave in our cross-correlations, we used the procedure developed by Takagi et al. (2014) to separate the body and the Rayleigh wave using the ZR and RZ components of the cross-correlations. Finally, Green's function was retrieved from the Rayleigh wave cross-correlation, using Eq. 3. The group velocity was measured using the Rayleigh wave Green's function. The group velocity was obtained using the multiple-filter technique of Dziewonski et al. (1969), which consists of applying a narrow band-pass filter to determine the group velocity. Figure 2 shows the Rayleigh wave dispersion curve obtained from applying the SPAC method and seismic interferometry

4.3. Velocity model estimation

We applied a joint inversion technique (Hayashida et al., 2019) to solve the obtained dispersion curve, which includes the phase and group velocity, as an iterative method to solve a nonlinear problem. In the inversion process, we used different initial models in which the P-wave velocity, the number of layers, and thickness of the layers were considered. The mismatch value (misfit) was determined for each calculated profile. the shear wave velocity was calculated from the dispersion curve, while the P velocity was defined using a linear relation from the S-wave velocity. And the density of the layer was obtained using the relation established by Kitsunezaki (1990).

The final velocity model is composed of five layers; overlying a homogeneous half-space. The model depth extends 3.5 km below the surface of the San Miguel volcano with P-wave velocities from 2.3 to 7.1 km/s and an S-wave velocity of 0.9–5.5 km/s (Figure 3). The velocity of the deepest layer is consistent with the local velocity model of El Salvador established by Marroquín (1998). The calculated velocity model presents a higher resolution in the shallower layers than the local velocity model of El Salvador. The effects of the sedimentary layers in the volcanic structure are observed, which causes low velocities in the shallow layers in our velocity model.

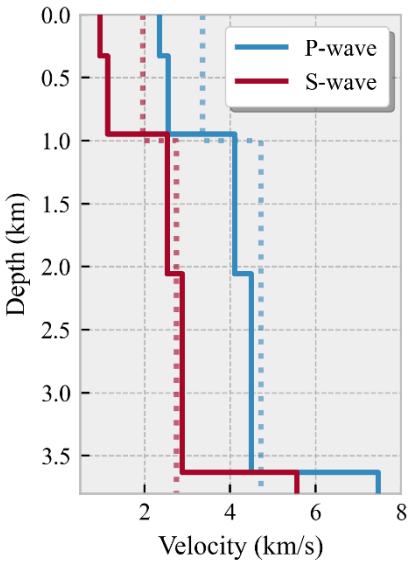

Figure 3. P-wave and S-wave velocity model computed for the San Miguel volcano. The dotted line represents the local velocity model of El Salvador

4.4 Earthquake location

We located some earthquakes associated with the volcano. The waveform shape was considered to discriminate seismicity associated with tectonics sources.

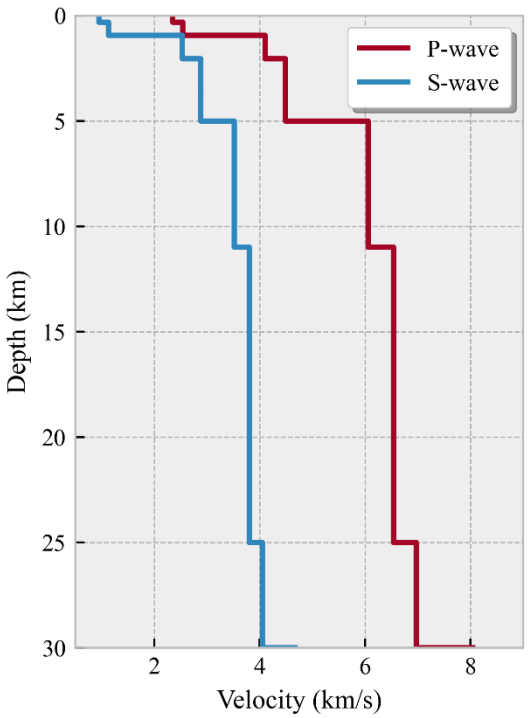

Figure 4. Velocity model used in the earthquake location

We focused the analysis on Volcano-Tectonic (VT) earthquakes due to their impulse P-wave arrivals. Considering the frequency content of the VT earthquakes and the waveform shape, we selected from our data three earthquakes and used them as templates to determine similar earthquakes.

The events were chosen using the open-source Repeating Earthquakes Detector in Python (RedPy) tool (Hotovec-Ellis et al., 2016). The tool detected 15 signals considered repeating earthquakes from one day-length data.

We manually picked the P-phase arrivals in the detected events using SEISAN software (Havskovet al., 1999) and the obtained velocity model. The bottom layer in our estimated velocity model is a half-space with low resolution, so we combined the bottom of the fourth layer of our velocity model with the top of the local velocity model of El Salvador to eliminate this ambiguity. Figure 4 shows the combined velocity structure.

In the location procedure, some difficulties were found due to ambiguous phase arrivals and complex waveform patterns. The complexity augmented considerably for distant stations, in which the SNR was low. Due to epicenter determination being carried out with only four stations, a phase misinterpretation could result in significantly significant errors.

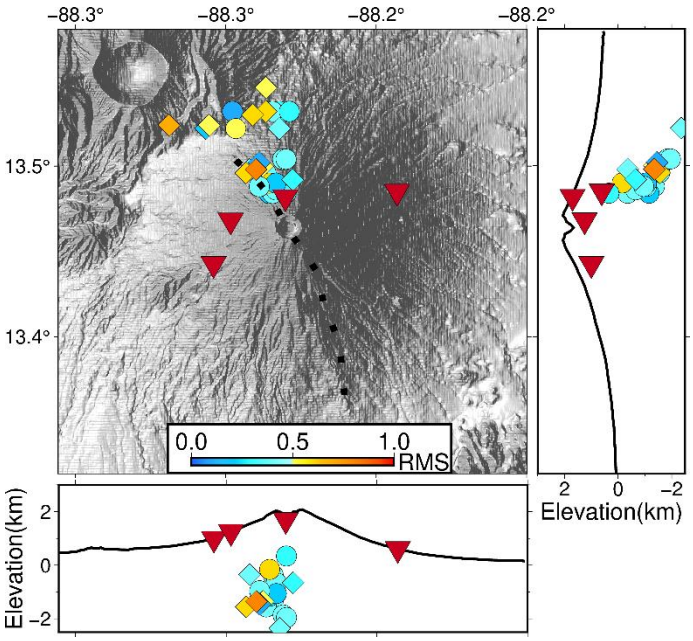

Figure 5. Located seismicity around San Miguel volcano. Inverted triangles represent seismic stations. The circles represent the location of seismic events using the proposed velocity model; the diamonds used the local velocity model proposed by Marroquín (1998). The dotted line indicates the San Miguel Fault Zone

The epicenter locations showed a tighter clustering of events located on the northern flank of the San Miguel volcano. The epicenters show a focus distribution; all are beneath the volcanic building with a shallow depth of about 1.5–3.0 km (Figure 5). The location of earthquakes in the volcano's northern flank is consistent with the deformation zone in the San Miguel volcano, known as San Miguel Fault Zone. We also located the selected events using the velocity model proposed by Marroquín (1998) to discuss the location differences. While there is no difference between epicenter locations, the main difference is observed in depth. There is an increment of the scatter for the events calculated with the previous velocity model, possibly due to the difference of shallow layers of the models. The lack of clusters is more evident in depth.

5. CONCLUSIONS

In this investigation, seismic ambient noise records in the San Miguel volcano were studied; the analyzed data included four months of continuous measurements recorded by four broadband stations covering a distance of 1.5 to 5.5 km around the volcano. We investigated the structural properties of the San Miguel volcano by estimating the Rayleigh-wave dispersion curve using the SPAC method and SI. Our seismic ambient noise analysis provided the first velocity model for the San Miguel volcano, in which few previous geophysical studies exist. The obtained velocity model is composed of four sedimentary layers (S-wave velocities of 0.9–2.8 km/s; P-wave velocities of 2.3–4.4 km/s) overlying a half-space layer.
Implementing the obtained velocity model resulted in better-constrained locations and depths in the analyzed seismicity. The high seismicity found in the northern flank of the San Miguel volcano is consistent with the location of the San Miguel Fault Zone. The information about this seismicity can represent an improvement in monitoring the San Miguel volcano, in which an accurate seismic-event location can represent critical information to its precursory and eruptive activity

ACKNOWLEDGEMENTS

Foremost, I would like to express my sincere gratitude to my research supervisor, Dr. Takumi Hayashida, for providing me with invaluable guidance throughout this research. It was a great privilege to develop this investigation under his direction. I want to share my gratitude to all the professors of IISEE/BRI for their continuous guidance and valuable assistance during my one-year study in Japan. Thanks for the academic advice and the teachings about scientific research and life.

REFERENCES

Aki, K. (1957). Bulletin of the Earthquake Research Institute, 35, 415–456.
Aki, K. (1965). Geophysics, 30(4), 665–666.
Bensen, G. D., Ritzwoller, M. H., Barmin, M. P., Levshin, A. L., Lin, F., Moschetti, M. P., Shapiro, N. M., & Yang, Y. (2007). Geophysical Journal International, 169(3), 1239–1260.
Dziewonski, A., Bloch, S., & Landisman, M. (1969). Bulletin of the Seismological Society of America, 59(1), 427–444.
Ekström, G., Abers, G. A., & Webb, S. C. (2009). Geophysical Research Letters, 36(18).
Havskov, J., & Ottemöller, L. (1999). Seismol. Res. Lett., 70(5), 532–534.
Hayashida, T., & Yokoi, T. (2019). Japan Association for Earthquake Engineering, 19(5), 111–124.
Hotovec-Ellis, A. J., & Jeffries, C. (2016). Seismological Society of America Annual Meeting.
Marroquín, G. (1998). Seismic properties of the crust in the volcanic chain of El Salvador C.A.
Takagi, R., Nakahara, H., Kono, T., & Okada, T. (2014). Journal of Geophysical Research: Solid Earth, 119(3), 2005–2018.
Wapenaar, K., & Fokkema, J. (2006). Geophysics, 71(4), SI33–SI46.